N65-82181

E-154

CP-1

TURBULENT FLOW IN A CIRCULAR TUBE WITH ARBITRARY INTERNAL HEAT SOURCES AND WALL HEAT TRANSFER

By R. Siegel and E. M. Sparrow, Associate Members, ASME

NASA, Lewis Research Center, Cleveland, Ohio

ABSTRACT

An analysis has been carried out to determine the heat transfer characteristics for turbulent flow of a heat generating fluid in a circular tube with wall heat transfer. The internal heat generation is uniform over the tube cross section, but may vary longitudinally in an arbitrary manner. The wall heat transfer may also vary in an arbitrary way in the longitudinal direction. The analysis applies along the entire length of the tube, that is, in thermal entrance as well as fully-developed regions. The fluid is assumed to have a fully developed turbulent velocity profile throughout the length of the pipe. Numerical results are presented for fluids with Prandtl numbers ranging from 0.7 to 100 for Reynolds numbers from 50,000 to 500,000. The extension of the results to include radial heat source variations is indicated.

NOMENCLATURE

c_p specific heat at constant pressure

D_n coefficients in series expansion of temperature for case of internal heat sources; D_n', coefficients when heat source is a function of radial position

d tube diameter, $2r_o$

E_n coefficients in series expansion of wall temperature for case of internal heat sources, $D_n \varphi_n(r_o^+)$

F_n coefficients in series expansion of wall temperature for case of wall heat transfer

$G(r^+)$ fully developed temperature distribution for case of uniform wall heat flux

$H(r^+)$ fully developed temperature distribution for case of uniform internal heat generation

h local heat transfer coefficient

k thermal conductivity

(3) McChugney 3/8/65 56/100
TMA#

$M(r^+)$ fully developed temperature distribution for case of heat sources dependent on r

Nu local Nusselt number, hd/k

Pr Prandtl number, ν/α

Q rate of internal heat generation per unit volume

q local heat transfer rate per unit area at tube wall

r radial coordinate measured from tube centerline; r_o, tube radius

r^+ dimensionless radial coordinate, $r\sqrt{\tau_o/\rho}/\nu$; r_o^+ dimensionless tube radius, $r_o\sqrt{\tau_o/\rho}/\nu$

Re Reynolds number, $\bar{u}d/\nu$

T absolute temperature; T_w, absolute wall temperature; T_b, absolute bulk fluid temperature

t temperature; t_o, temperature of fluid entering tube (a constant); t^*, difference temperature defined in equation (5); t_b, bulk fluid temperature; t_w, tube wall temperature

u fluid velocity in the x-direction; $\bar{u}$, mean fluid velocity

u^+ dimensionless velocity in x-direction, $u/\sqrt{\tau_o/\rho}$

x axial coordinate measuring distance from tube entrance

x^+ dimensionless axial coordinate, x/d

$\bar{x}$ dummy integration variable

y radial coordinate measuring distance inward from tube wall, $r_o - r$

y^+ dimensionless coordinate, $y\sqrt{\tau_o/\rho}/\nu$

α molecular diffusivity for heat, $k/\rho c_p$

β^2 eigenvalues of equation (17a)

γ dimensionless total thermal diffusivity, $(\alpha + \epsilon_h)/\nu$

ϵ_h, ϵ_m eddy diffusivities for heat and momentum

ν kinematic viscosity

ρ fluid density

τ_o shear stress at tube wall

φ eigenfunctions of equation (17a)

ψ function of x given by equation (16)

Subscripts:

fd denotes fully developed heat transfer condition

Q denotes situation where $Q \neq 0$ and $q = 0$

q denotes situation where $q \neq 0$ and $Q = 0$

INTRODUCTION

Flowing fluids with internal heat generation are found in many sectors of modern technology. Such flows may occur, for example, in fluid-fueled nuclear reactors and chemical process equipment. The basic flow passage in many of these systems is the circular tube, and it is this configuration which is selected for analysis here.

Specifically, we are concerned with turbulent pipe flows in which the internal heat generation is uniform across the section, but which may vary in an arbitrary manner along the length. Furthermore, the heat transfer at the tube wall is also permitted to take on an arbitrary longitudinal variation. An example of a situation where such variations may occur is in a nuclear reactor core in which the neutron flux varies with position.

The findings of the analysis can be used to calculate the heat transfer characteristics over the entire length of the passage, that is, in the thermal entrance as well as far downstream. Numerical results are provided over the Reynolds number range from 50,000 to 500,000 for Prandtl numbers varying from 0.7 to 100.

Previous analyses (1,2,3) of turbulent pipe flows with internal heat generation have been confined to the condition of fully developed heat transfer, and hence, the results pertain to the portion of pipe beyond the thermal entrance region. Also, these investigations were carried out under the restrictions that the internal heat generation and wall heat transfer are both longitudinally uniform. Laminar pipe flows have, however, lent themselves more readily to analysis. Results applicable over the entire pipe length have been given (4) for the general situation where the internal heat generation takes on arbitrary longitudinal and radial variations, while the wall heat transfer varies arbitrarily along the length. Of course, turbulent flows are of greater importance as they are almost always encountered in practice.

GENERAL ANALYTICAL CONSIDERATIONS

The system to be analyzed is pictured schematically on figure 1. Our attention is directed to the portion of the tube to the right of $x = 0$ where the fluid simultaneously experiences an internal heat generation $Q(x)$ and a wall heat transfer $q(x)$. The functions Q and q are permitted arbitrary variations with x. The fluid, moving from left to right, possesses a fully developed turbulent velocity profile which is unchanging with length. The temperature across the entrance section, $x = 0$, is taken to be uniform at the value t_o. It is desired to determine the heat transfer characteristics of the fluid at all positions along the tube.

The starting point of our study is the equation expressing conservation of energy for axially symmetric turbulent flow in a pipe. For fully developed hydrodynamic conditions, this may be written as

$$u \frac{\partial t}{\partial x} = \frac{1}{r} \frac{\partial}{\partial r}\left[r(\alpha + \epsilon_h) \frac{\partial t}{\partial r}\right] + \frac{Q}{\rho c_p} \tag{1}$$

where α and ϵ_h represent respectively the molecular and eddy diffusivities for heat. To obtain the energy equation in this form, it has been assumed that the fluid properties are constant, and that viscous dissipation and axial heat diffusion are both negligible compared to heat diffusion in the radial direction.

Since equation (1) is linear in the temperature t, we are able to separate the general problem which includes both internal heat sources and wall heat transfer into two simpler situations in the following way: (a) A problem where there is an internal heat generation Q in an insulated tube $(q = 0)$. For this case, the temperature is designated as t_Q. (b) A problem where there is a wall heat transfer q without

E-154

internal heat generation $(Q = 0)$. In this instance we denote the temperature by t_q. Then, from the linearity of the energy equation, the temperature in the combined problem is simply given by

$$t = t_Q + t_q \tag{2}$$

The governing equations and boundary conditions for t_Q and t_q may be written as follows:

$$u \frac{\partial t_Q}{\partial x} = \frac{1}{r} \frac{\partial}{\partial r}\left[r(\alpha + \epsilon_h) \frac{\partial t_Q}{\partial r}\right] + \frac{Q}{\rho c_p} \tag{3a}$$

$$\left.\begin{aligned} &\partial t_Q/\partial r = 0 \quad \text{at} \quad r = r_o \quad \text{(insulated wall)} \\ &\partial t_Q/\partial r = 0 \quad \text{at} \quad r = 0 \quad \text{(symmetry)} \\ &t_Q = t_{Q,o} \quad \text{at} \quad x = 0 \quad \text{(entrance condition)} \end{aligned}\right\} \tag{3b}$$

and

$$u \frac{\partial t_q}{\partial x} = \frac{1}{r} \frac{\partial}{\partial r}\left[r(\alpha + \epsilon_h) \frac{\partial t_q}{\partial r}\right] \tag{4a}$$

$$\left.\begin{aligned} &\partial t_q/\partial r = q/k \quad \text{at} \quad r = r_o \ \text{(specified heat flux)} \\ &\partial t_q/\partial r = 0 \quad \text{at} \quad r = 0 \ \text{(symmetry)} \\ &t_q = t_{q,o} \quad \text{at} \quad x = 0 \ \text{(entrance condition)} \end{aligned}\right\} \tag{4b}$$

where $t_{Q,o}$ and $t_{q,o}$ are chosen so that

$$t_o = t_{Q,o} + t_{q,o} \tag{2a}$$

The two problems as defined by equations (3) and (4) will be analyzed separately.

We begin by studying the problem of a flow with internal heat sources in an insulated tube, that is, t_Q. First, consideration is given to the situation of uniform heat sources, and a solution is obtained which applies both in the entrance and fully developed regions. Then, these results are generalized to the case where there are arbitrary variations of the heat sources along the length of the tube. Next, the results for the problem of uniform wall heat transfer with no heat sources, originally given in reference (5), are reviewed and generalized to apply for arbitrary longitudinal variations of heat flux. The linear combination of these solutions is then made to yield results for the general case of arbitrary longitudinal variations in both internal heat sources and wall heat flux. Extension of the analysis to the situation of radially nonuniform heat sources is made in the last section of the report.

The eddy diffusivity which appears in equations (3a) and (4a) bears a word of discussion. Current knowledge of the relationship between the eddy diffusivity for heat, ϵ_h, and the eddy diffusivity for momentum, ϵ_m, is still in a state of uncertainty. However, it appears that for the Prandtl numbers of this study, $0.7 \leq Pr \leq 100$, the choice of $\epsilon_h = \epsilon_m$ is not unreasonable. Previous application of this assumption has led to excellent heat transfer predictions over this Prandtl number range.

UNIFORM INTERNAL HEAT SOURCES IN AN INSULATED TUBE

For uniform heating conditions, it is well-known that as the flow proceeds farther and farther down the pipe, the heat transfer characteristics approach more and more closely to a limiting condition. This limit is termed the fully developed heat transfer situation and will be denoted by the subscript fd. Taking cognizance of the fully developed condition, we choose to write the temperature distribution t_Q as the following sum

$$t_Q = t_{Q,fd} + t_Q^* \tag{5}$$

t_Q^* is seen to be a difference temperature which plays an important role in the entrance region and approaches zero as x becomes large. We now proceed to solve separately for $t_{Q,fd}$ and t_Q^*.

<u>The fully developed solution</u>. - Since energy conservation must everywhere be obeyed, it is necessary that $t_{Q,fd}$ satisfy equation (3a), that is,

$$u \frac{\partial t_{Q,fd}}{\partial x} = \frac{1}{r} \frac{\partial}{\partial r}\left[r(\alpha + \epsilon_m) \frac{\partial t_{Q,fd}}{\partial r}\right] + \frac{Q}{\rho c_p} \tag{6}$$

where Q is now a constant and ϵ_h has been replaced by ϵ_m. A characteristic of the fully developed situation for uniform heat sources is that the temperature at all points in the cross section rises in a linear fashion along the pipe. Expressed in mathematical terms, the condition becomes

$$\frac{\partial t_{Q,fd}}{\partial x} = \text{constant} = \frac{Q}{\rho \bar{u} c_p} \tag{7a}$$

or alternately

$$\frac{t_{Q,fd} - t_{Q,o}}{Q r_o^2/k} = \frac{4}{RePr}\,\frac{x}{d} + H(r) \tag{7b}$$

E-154

The radial distribution $H(r)$ must, of course, satisfy the conservation of energy equation (6). Substituting (7b) into (6) and introducing dimensionless variables, the governing equation for H is found to be

$$\frac{2u^+}{RePr} = \frac{r_o^+}{r^+}\,\frac{d}{dr^+}\left[r^+ \gamma \frac{dH}{dr^+}\right] + \frac{1}{(Pr) r_o^+} \tag{8}$$

where u^+ and r^+ are the dimensionless counterparts of u and r as given in the symbol list, and γ represents a dimensionless diffusivity defined as

$$\gamma = \frac{\alpha + \epsilon_m}{\upsilon} = \frac{1}{Pr} + \frac{\epsilon_m}{\upsilon}$$

The boundary conditions on H are found from equation (3b) to be

$$dH/dr^+ = 0 \quad \text{at} \quad r^+ = 0 \quad \text{and} \quad r^+ = r_o^+ \tag{8a}$$

To obtain solutions of equation (8), it is necessary that the variation of u^+ and γ with r^+ be specified. The turbulent velocity distribution is given by the following equations (ref. 6).

$$\frac{du^+}{dy^+} = \frac{1}{1 + (0.124)^2\, u^+ y^+ \left[1 - e^{-(0.124)^2\, u^+ y^+}\right]}, \qquad 0 \le y^+ \le 26 \tag{9a}$$

$$u^+ = \frac{1}{0.36} \ln\left(\frac{y^+}{26}\right) + 12.8493, \qquad 26 \le y^+ \tag{9b}^*$$

where $y^+ = r_o^+ - r^+$, while γ is evaluated from (ref. 5)

$$\gamma = \frac{1}{Pr} + (0.124)^2\, u^+ y^+ \left[1 - e^{-(0.124)^2\, u^+ y^+}\right], \qquad 0 < y^+ < 26 \tag{10a}$$

$$\gamma = \frac{1}{Pr} + 0.36 y^+ \left(1 - y^+/r_o^+\right) - 1, \qquad y^+ > 26 \tag{10b}$$

*The constant 12.8493, evaluated to higher accuracy for the purpose of this investigation, differs slightly from that of reference 6.

The value of γ at $y^+ = 26$ is taken as the average of equations (10a) and (10b). The minus one term appearing on the right side of equation (10b) is retained for $26 < y^+ < r_o^+/2$ and is deleted for larger values of y^+.

With these expressions for u^+ and γ, we can proceed with the integration of equation (8) in order to find H. An analytical solution was not possible and a numerical technique (Kutta-Runge method) had to be employed. Solutions were carried out on an IBM 653 electronic computer for Reynolds numbers of 50,000; 100,000; and 500,000 for Prandtl numbers of 0.7, 1, 10, and 100. The values of H thus obtained provide, in conjunction with equation (7b), the complete solution for the fully developed situation. Space considerations preclude tabulation of the solutions here, but they are available as IBM listings.

A result of practical engineering importance is the wall-to-bulk temperature difference for the fully developed situation. First, the bulk temperature is introduced by its definition

$$t_{Q,b} - t_{Q,o} = \frac{Q}{\rho \bar{u} c_p} x = \frac{Q r_o^2}{k} \frac{4(x/d)}{RePr} \tag{11}$$

Then, substituting into equation (7b) and evaluating H at the tube wall $(r^+ = r_o^+)$ we find

$$\frac{(t_{Q,w} - t_{Q,b})_{fd}}{Q r_o^2/k} = H(r_o^+) \tag{12}$$

Using the numerical results for $H(r_o^+)$, the dimensionless wall-to-bulk temperature difference has been plotted on figure 2 as a function of the Reynolds and Prandtl numbers.

We will make further use of the fully developed solution in later sections.

<u>The thermal entrance region</u>. - According to equation (5), the temperature distribution in the thermal entrance region is found by adding the difference temperature t_Q^* to the fully developed temperature $t_{Q,fd}$. Having determined $t_{Q,fd}$, we now turn our attention to t_Q^*.

To find the governing equation for t_Q^*, we introduce equation (5) into the conservation of energy principle (3a). Then, taking account of the fact that $t_{Q,fd}$ satisfies (6), it follows that t_Q^* must obey

$$\frac{u^+}{2}\frac{\partial t_Q^*}{\partial x^+} = \frac{r_o^+}{r^+}\frac{\partial}{\partial r^+}\left[r^+\gamma\,\frac{\partial t_Q^*}{\partial r^+}\right] \tag{13}$$

where again dimensionless variables have been used. It is interesting to observe that the heat source term does not appear in equation (13).

The boundary conditions on t_Q^* may be derived from equations (3b), in conjunction with (5), giving

$$\partial t_Q^*/\partial r^+ = 0 \quad \text{at} \quad r^+ = 0 \quad \text{and} \quad r^+ = r_o^+ \tag{14a}$$

and

$$\left.\begin{aligned} t_Q^* &= t_{Q,o} - t_{Q,fd} \\ \text{or} \qquad \frac{t_Q^*}{Qr_o^2/k} &= -H(r) \end{aligned}\right\} \quad \text{at} \quad x = 0 \tag{14b}$$

where we have also used equation (7b) in finding the last expression.

We seek a solution for t_Q^* in the form of a product

$$\frac{t_Q^*}{Qr_o^2/k} = D\varphi(r^+)\ \psi(x^+) \tag{15}$$

where ψ and φ, respectively, depend on x^+ and r^+ alone. By substituting into the differential equation (13), we find that

$$\psi = e^{-4\beta^2 x^+/Re} \tag{16}$$

$$\frac{d}{dr^+}\left(r^+\gamma\ \frac{d\varphi}{dr}\right) + \left(\frac{2\beta^2}{Re}\ \frac{r^+}{r_o^+}\ u^+\right)\varphi = 0 \tag{17a}$$

where $-\dfrac{2\beta^2}{Re}$ is the separation constant arising from the product solution. From (14a), the boundary conditions on equation (17a) are

$$d\varphi/dr^+ = 0 \quad \text{at} \quad r^+ = 0 \quad \text{and} \quad r^+ = r_o^+ \tag{17b}$$

Equations (17a) and (17b) comprise an eigenvalue problem of the Sturm-Liouville type. Solutions are possible only for a discrete, though infinite, set of β values. Hence, the solution for t^* can be written as

$$\frac{t_Q^*}{Qr_o^2/k} = \sum_{n=0}^{\infty} D_n \varphi_n(r^+) e^{-4\beta_n^2 x^+/Re} \tag{15a}$$

where β_n are the eigenvalues and φ_n are the corresponding eigenfunctions of equations (17a) and (17b). Since the values of r_o^+ and γ in equation (17a) depend on the Reynolds and Prandtl numbers, there will be a different set of eigenvalues associated with each choice of these parameters. Utilizing numerical integration, the first six eigenvalues and eigenfunctions have been found for the same Reynolds and Prandtl numbers previously mentioned. The eigenvalues are listed in table I, while the corresponding eigenfunctions are available as IBM tabulations.

The coefficients D_n of equation (15a) are still to be determined. Applying the boundary condition at the tube entrance as given by equation (14b), we have

$$\sum_{n=0}^{\infty} D_n \varphi_n = -H(r^+) \tag{18a}$$

From this, it follows immediately from the properties of the Sturm-Liouville system that

$$D_n = \frac{\int_0^{r_o^+} [-H(r^+)]\, r^+ u^+ \varphi_n \, dr^+}{\int_0^{r_o^+} r^+ u^+ \varphi_n^2 \, dr^+} \tag{18b}$$

It is seen that the computation of the D_n involves an integration of the fully developed temperature distribution. With the β_n, φ_n, and D_n determined, the difference temperature t_Q^* is known from equation (15a), and we may now proceed with the complete solution of the problem.

The complete temperature solution. - Combining the results of the preceeding sections in accordance with equation (5), we are able to write an expression for the temperature distribution which applies both in the entrance and fully developed regions, that is,

$$\frac{t_Q - t_{Q,o}}{Qr_o^2/k} = \frac{4}{RePr}\frac{x}{d} + H(r^+) + \sum_{n=0}^{\infty} D_n \varphi_n(r^+) e^{-\frac{4\beta_n^2}{Re}\frac{x}{d}} \tag{19}$$

Of particular practical interest is the difference between the wall and bulk temperatures at all stations along the pipe. Evaluating equation (19) at the wall ($r^+ = r_o^+$) and substituting the bulk temperature from equation (11) yields

$$\frac{t_{Q,w} - t_{Q,b}}{Qr_o^2/k} = H(r_o^+) + \sum_{n=0}^{\infty} D_n \varphi_n(r_o^+) e^{-\frac{4\beta_n^2}{Re}\frac{x}{d}} \tag{20}$$

A convenient rephrasing of this result may be carried out by introducing the fully developed wall-to-bulk temperature difference from (12), giving

$$\frac{t_{Q,w} - t_{Q,b}}{(t_{Q,w} - t_{Q,b})_{fd}} = 1 + \frac{\sum_{n=0}^{\infty} E_n e^{-\frac{4\beta_n^2}{Re}\frac{x}{d}}}{H(r_o^+)} \tag{20a}$$

where the product $D_n \varphi_n(r_o^+)$ has been abbreviated by E_n. Numerical values of E_n have been listed in table II as a function of the Reynolds and Prandtl numbers, while $H(r_o^+)$ may be read directly as the ordinate of figure 2. Using these numerical data, the ratio of temperature differences given by (20a) has been plotted on figures 3(a) and 3(b) as a function of distance along the tube for parametric values of the Reynolds and Prandtl numbers*. The information given on these plots, used in conjunction with figure 2, permits rapid evaluation of the wall-to-bulk temperature difference at various stations along the tube.

We can define a thermal entrance length as the heated length required for $(t_{Q,w} - t_{Q,b})$ to approach to within 5 percent of the fully developed value. A dashed line has been drawn on figures 3(a) and 3(b) to facilitate finding the entrance length.

*The curves do not extend all the way to $x = 0$ because the series has been truncated.

E-154

CP-2 back

So, for example, for Re = 50,000 and Pr = 100, the entrance length is 15 diameters; while for Re = 50,000 and Pr = 0.7, the entrance length is 21 diameters.. A very significant finding is that, especially for high Prandtl numbers, these entrance lengths are substantially greater than those encountered in turbulent pipe flow with uniform wall heat transfer or uniform wall temperature. These differences in entrance length will be emphasized in a later section when the results for uniform wall heat flux are given.

ARBITRARY LONGITUDINAL HEAT SOURCE VARIATIONS IN AN INSULATED TUBE

We now proceed to generalize these results to apply for arbitrary variations of the internal heat generation along the tube. For the purposes of analysis, suppose that $Q(x)$ can be represented as in figure 4. Envision for the moment an elementary heating process in which there is no internal heat generation up to a position $\bar{x}$; then, beyond $\bar{x}$, there occurs a uniform internal heating of magnitude dQ. The temperature response to such a process can be found by applying equation (19).

$$\frac{t_Q - t_{Q,o}}{r_o^2/k} = dQ\left[\frac{4\,\frac{(x - \bar{x})}{d}}{\mathrm{RePr}} + H(r^+) + \sum_{n=0}^{\infty} D_n\varphi_n\, e^{-\frac{4\beta_n^2}{\mathrm{Re}}\frac{(x-\bar{x})}{d}}\right], \qquad x \geq \bar{x} \tag{21}$$

This elementary heating process can be considered as a differential step in the heat source variation pictured on figure 4. By integrating the separate effects of these elementary steps, we are able to find the temperature distribution at any position corresponding to a prescribed upstream variation of $Q(x)$. The integral of the right side can be rephrased into a more convenient form by integrating by parts. The result of this operation is

$$\frac{t_Q - t_{Q,o}}{r_o/k} = \frac{2}{\mathrm{RePr}}\int_0^x Q(\bar{x})d\bar{x} - \frac{2}{\mathrm{Re}}\sum_{n=0}^{\infty} D_n\varphi_n\beta_n^2\int_0^x Q(\bar{x})\, e^{-\frac{4\beta_n^2}{\mathrm{Re}}\frac{(x-\bar{x})}{d}}d\bar{x} \tag{22}$$

Now, turning to the wall-to-bulk temperature difference, we evaluate equation (22) at $r^+ = r_o^+$ and introduce the bulk temperature by its definition

$$t_{Q,b} = t_{Q,o} + \frac{(d/k)}{RePr} \int_0^x Q(\bar{x})d\bar{x} \tag{23}$$

finally giving,

E-154

$$t_{Q,w} - t_{Q,b} = -\frac{2r_o/k}{Re} \sum_{n=0}^{\infty} E_n \beta_n^2 \int_0^x Q(\bar{x})\, e^{-\frac{4\beta_n^2}{Re} \frac{(x-\bar{x})}{d}} d\bar{x} \tag{24}$$

Numerical values of E_n and β_n^2 are given in tables I and II, so that the integration can be carried out (either analytically or numerically) for any prescribed variation of the internal heat generation $Q(\bar{x})$.

WALL HEAT TRANSFER WITHOUT INTERNAL HEAT GENERATION

Uniform wall heat flux. - An analysis of turbulent pipe flow with uniform wall heat flux has been given in reference 5 and only the results need be reviewed here.

First, for the fully developed heat transfer condition, the wall-to-bulk temperature difference corresponding to the uniform heating at the wall has been plotted on figure 5 for the same Reynolds and Prandtl number ranges as heretofore considered*. It may be noted that the ordinate is proportional to the reciprocal of the fully developed Nusselt number, which has its usual definition

$$Nu_{fd} = \frac{h_{fd}d}{k}, \qquad h_{fd} = \frac{q}{(t_{q,w} - t_{q,b})_{fd}} \tag{25}$$

while the bulk temperature for uniform heat flux is given by

$$t_{q,b} - t_{q,o} = \frac{qr_o}{k} \frac{8(x/d)}{RePr} \tag{26}$$

Unpublished experimental data of Presler and Loeffler (7) also appear on figure 5 and show excellent agreement with the theory. The fluid properties appearing in the experimental correlation were evaluated at the film temperature.

*The results of reference 5 have been extended to cover the $Pr = 1$ case.

Results for the wall-to-bulk temperature difference which apply all along the tube are given in the form of the ratio

$$(t_{q,w} - t_{q,b})/(t_{q,w} - t_{q,b})_{fd}$$

which is plotted on figures 6(a) and 6(b) as a function of x/d for parametric values of the Reynolds and Prandtl numbers. The use of figure 6, in conjunction with figure 5, permits rapid computation of those temperature results of greatest practical interest. The ordinate of figure 6 can also be recognized as the ratio

$$Nu_{fd}/Nu$$

where Nu is the local Nusselt number defined by equation (25) with subscripts fd deleted.

For this situation of uniform wall heat flux, a thermal entrance region can be defined as the length required for $(t_{q,w} - t_{q,b})$ to approach within 5 percent of its fully developed value, or alternately, as the length required for the Nusselt number to approach within 5 percent of its fully developed value. A dashed line has been drawn on figure 6 to aid in determining the thermal entrance lengths. Comparison of figure 6 with figure 3, especially for the high Prandtl numbers, verifies our previous statement about the considerably greater entrance lengths associated with the case of internal heat generation. Further, it is interesting to observe that the Reynolds number appears to play a much greater role in determining the entrance lengths for the heat generation case.

While the important results of reference 5 have been graphed on figures 5 and 6, it will also be useful to give their analytical representation as follows

$$\frac{t_{q,w} - t_{q,o}}{qr_o/k} = \frac{8(x/d)}{RePr} + G(r_o^+) + \sum_{n=0}^{\infty} F_n \, e^{-\frac{4\beta_n^2}{Re}\frac{x}{d}} \tag{26}$$

where β_n^2 and F_n are listed in tables I* and III, respectively, and $G(r_o^+)$ is read directly from the ordinate of figure 5.

Arbitrary wall heat flux. - Following a procedure identical to that outlined previously, the results for the uniform heat flux case as expressed by equation (26) may be generalized to apply to arbitrary longitudinal variations $q(x)$. First considering an elementary heating process and then integrating the effects of many such processes, we find that

$$t_{q,w} - t_{q,b} = -\frac{2}{k\ \mathrm{Re}} \sum_{n=0}^{\infty} F_n \beta_n^2 \int_0^x q(\bar{x})\, e^{-\frac{4\beta_n^2}{\mathrm{Re}} \frac{(x-\bar{x})}{d}}\, d\bar{x} \tag{27}$$

where

$$t_{q,b} = t_{q,o} + \frac{4}{k\ \mathrm{RePr}} \int_0^x q(\bar{x})\, d\bar{x} \tag{28}$$

Equation (27) gives the wall temperature at any position for a prescribed upstream variation in wall heat flux. Inasmuch as the constants β_n^2 and F_n are available in tables I and III, the integration can be carried out as soon as the variation of q is given.

COMBINED INTERNAL SOURCES AND WALL HEAT TRANSFER

We can now proceed to write the solution for the situation where internal heat generation and wall heat transfer occur simultaneously. According to equation (2), results for this combined problem are found by adding the contributions due to each of the separate problems.

The most important result of practical interest is the wall temperature variation corresponding to given heating conditions. To compute this, we apply equation (2) to the wall and bulk temperatures

$$t_w = t_{Q,w} + t_{q,w} \qquad t_b = t_{Q,b} + t_{q,b} \tag{29}$$

---

*The β_n^2 values listed here are slightly refined compared with those of ref. 5.

Then, subtracting the second of these from the first gives

$$t_w - t_b = (t_{Q,w} - t_{Q,b}) + (t_{q,w} - t_{q,b}) \tag{30a}$$

Consideration is first given to the situation where both the internal heating and the wall heat flux are uniform along the length. For these circumstances, equation (30a) can be recast into a form more convenient for rapid calculations as follows:

$$t_w - t_b = \left[\frac{t_{Q,w} - t_{Q,b}}{(t_{Q,w} - t_{Q,b})_{fd}}\right](t_{Q,w} - t_{Q,b})_{fd} + \left[\frac{t_{q,w} - t_{q,b}}{(t_{q,w} - t_{q,b})_{fd}}\right](t_{q,w} - t_{q,b})_{fd} \tag{30b}$$

where the subscript fd denotes the fully developed situation. Numerical values of the first square bracket may be read directly from figures 3(a) and 3(b); while the second square bracket is read directly from figures 6(a) and 6(b). The fully developed temperature differences $(t_{Q,w} - t_{Q,b})_{fd}$ and $(t_{q,w} - t_{q,b})_{fd}$ are found from figures 2 and 5, respectively. The bulk temperature for the situation of combined uniform heat generation and wall heating is computed from

$$t_b = t_o + \frac{4(x/d)}{RePr}\left[\frac{Qr_o^2}{k} + \frac{2qr_o}{k}\right] \tag{31}$$

So, with this information, equation (30b) may be easily evaluated to give the wall temperature at various stations along the tube.

Now, we turn to the situation where the internal heating and wall heat transfer vary in an arbitrary way along the length. Equation (30a) is then applied, and the temperature differences $(t_{Q,w} - t_{Q,b})$ and $(t_{q,w} - t_{q,b})$ are respectively evaluated from equations (24) and (27). The numerical values of β_n^2, E_n, and F_n needed in the computations are listed in tables I, II, and III, while the bulk temperature corresponding to the longitudinally nonuniform heating is given by

$$t_b = t_o + \frac{1}{k\ RePr}\left[4\int_0^x q(\bar{x})\ d\bar{x} + d\int_0^x Q(\bar{x})d\bar{x}\right] \tag{32}$$

Once the longitudinal variations are prescribed, equation (30a) may then be used to compute the wall temperature at various positions.

RADIAL VARIATIONS OF THE INTERNAL HEAT GENERATION

In this paper, numerical results have been provided for the case of internal heat sources which are uniform across the tube cross section. However, the results can be extended to heat sources which vary in the radial direction. In this instance, the fully developed temperature distribution is given by

$$\frac{t_{Q,fd} - t_{Q,o}}{\frac{2}{k}\int_0^{r_o} Q(r)r\ dr} = \frac{4}{RePr}\frac{x}{d} + M(r) \tag{33}$$

which is of a form similar to equation (7b). The function $M(r)$ must be found by integrating the equation

$$\frac{2u^+}{RePr} = \frac{r_o^+}{r}\frac{d}{dr^+}\left[r^+\gamma\frac{dM}{dr^+}\right] + \frac{r_o^+}{2Pr}\frac{Q(r^+)}{\int_0^{r_o^+} Q(r^+)r^+dr^+} \tag{34}$$

With $Q(r)$ specified, this can be solved numerically in the same manner and with the same boundary conditions as equation (8).

The eigenvalues and eigenfunctions arising in the solution of the difference temperature t_Q^* remain unchanged, but the D_n in equation (18b) now have to be evaluated using $-M(r^+)$ in place of $-H(r^+)$. Hence, for the difference temperature t_Q^*, we can write

$$\frac{t_Q^*}{\frac{2}{k}\int_0^{r_o} Qr\ dr} = \sum_{n=0}^{\infty} D_n'\varphi_n(r^+)\ e^{-\frac{4\beta_n^2x^+}{Re}} \tag{35}$$

where

$$D_n' = \frac{\int_0^{r_o^+}\left[-M(r^+)\right]r^+u^+\varphi_n\ dr^+}{\int_0^{r_o^+} r^+u^+\varphi_n^2dr^+} \tag{36}$$

These expressions can be evaluated for any prescribed radial heat source variation, and the extension to longitudinal variations proceeds in the same manner as described previously for uniform heat sources.

REFERENCES

1. Poppendiek, H. F., and Palmer, L. D.: "Forced Convection Heat Transfer in Pipes with Volume Heat Sources Within the Fluids" ORNL-1395, 1952.

2. Poppendiek, H. F.: "Forced-Convection Heat Transfer in Pipes with Volume-Heat Sources Within the Fluids." Chem. Eng. Progress Symposium Series No. 50, 1954, Nuclear Engineering, Part I, pp. 93-104.

3. Poppendiek, H. F., and Palmer, L. D.: Application of Temperature Solutions for Forced Convection Systems with Volume Heat Sources to General Convection Problems." ORNL-1933, 1955.

4. Sparrow, E. M., and Siegel, R.: "Laminar Tube Flow with Arbitrary Internal Heat Sources and Wall Heat Transfer." Nuclear Science and Engineering, vol. 4, no. 2, 1958, pp. 239-254.

5. Sparrow, E. M., Hallman, T. M., and Siegel, R.: "Turbulent Heat Transfer in the Thermal Entrance Region of a Pipe with Uniform Heat Flux." Applied Scientific Research, vol. 7, Section A, 1957, pp. 37-52.

6. Deissler, Robert G.: "Analysis of Turbulent Heat Transfer, Mass Transfer, and Friction in Smooth Tubes at High Prandtl and Schmidt Numbers," NACA Rep. 1210, 1955. (Supersedes NACA TN 3145.)

7. Personal Communication with A. E. Presler, and A. L. Loeffler, Jr., NASA Lewis Research Center.

E-154

CP-3 back

TABLE I. - LISTING OF EIGENVALUES, β_n^2

(a) Re = 50,000.

Pr	β_0^2	β_1^2	β_2^2	β_3^2	β_4^2	β_5^2
0.7	0	1387	3730	7040	11,330	16,600
1.0	0	1380	3705	6981	11,220	16,410
10.0	0	1366	3651	6850	10,960	15,950
100.0	0	1364	3645	6835	10,930	15,880

(b) Re = 100,000.

Pr	β_0^2	β_1^2	β_2^2	β_3^2	β_4^2	β_5^2
0.7	0	2545	6822	12,850	20,630	30,190
1.0	0	2538	6796	12,790	20,520	30,000
10.0	0	2524	6742	12,660	20,270	29,560
100.0	0	2522	6737	12,640	20,240	29,510

(c) Re = 500,000.

Pr	β_0^2	β_1^2	β_2^2	β_3^2	β_4^2	β_5^2
0.7	0	10,680	28,520	53,560	85,810	125,300
1.0	0	10,670	28,490	53,490	85,690	125,100
10.0	0	10,660	28,440	53,360	85,440	124,700
100.0	0	10,660	28,430	53,350	85,410	124,600

TABLE II. - VALUES OF THE COEFFICIENTS E_n

(a) Re = 50,000.

Pr	$-E_0$	$-E_1$	$-E_2$	$-E_3$	$-E_4$	$-E_5$
0.7	0	0.1753×10^{-3}	0.5039×10^{-4}	0.2405×10^{-4}	0.1422×10^{-4}	0.9719×10^{-5}
1.0	0	$.1242\times10^{-3}$	$.3616\times10^{-4}$	$.1752\times10^{-4}$	$.1055\times10^{-4}$	$.7362\times10^{-5}$
10.0	0	$.1293\times10^{-4}$	$.3973\times10^{-5}$	$.2071\times10^{-5}$	$.1379\times10^{-5}$	$.1093\times10^{-5}$
100.0	0	$.1328\times10^{-5}$	$.4263\times10^{-6}$	$.2377\times10^{-6}$	$.1734\times10^{-6}$	$.1576\times10^{-6}$

(b) Re = 100,000.

Pr	$-E_0$	$-E_1$	$-E_2$	$-E_3$	$-E_4$	$-E_5$
0.7	0	0.8775×10^{-4}	0.2454×10^{-4}	0.1128×10^{-4}	0.6421×10^{-5}	0.4180×10^{-5}
1.0	0	$.6186\times10^{-4}$	$.1742\times10^{-4}$	$.8076\times10^{-5}$	$.4640\times10^{-5}$	$.3056\times10^{-5}$
10.0	0	$.6323\times10^{-5}$	$.1831\times10^{-5}$	$.8799\times10^{-6}$	$.5304\times10^{-6}$	$.3708\times10^{-6}$
100.0	0	$.6388\times10^{-6}$	$.1892\times10^{-6}$	$.9353\times10^{-7}$	$.5879\times10^{-7}$	$.4341\times10^{-7}$

(c) Re = 500,000.

Pr	$-E_0$	$-E_1$	$-E_2$	$-E_3$	$-E_4$	$-E_5$
0.7	0	0.1781×10^{-4}	0.4789×10^{-5}	0.2114×10^{-5}	0.1158×10^{-5}	0.7194×10^{-6}
1.0	0	$.1249\times10^{-4}$	$.3366\times10^{-5}$	$.1489\times10^{-5}$	$.8174\times10^{-6}$	$.5094\times10^{-6}$
10.0	0	$.1256\times10^{-5}$	$.3405\times10^{-6}$	$.1519\times10^{-6}$	$.8421\times10^{-7}$	$.5310\times10^{-7}$
100.0	0	$.1259\times10^{-6}$	$.3428\times10^{-7}$	$.1537\times10^{-7}$	$.8581\times10^{-8}$	$.5459\times10^{-8}$

TABLE III. - VALUES OF THE COEFFICIENTS F_n

(a) Re = 50,000.

Pr	$-F_0$	$-F_1$	$-F_2$	$-F_3$	$-F_4$	$-F_5$
0.7	0	0.3507×10^{-2}	0.1848×10^{-2}	0.1278×10^{-2}	0.9842×10^{-3}	0.8209×10^{-3}
1.0	0	$.2505\times10^{-2}$	$.1342\times10^{-2}$	$.9486\times10^{-3}$	$.7480\times10^{-3}$	$.6409\times10^{-3}$
10.0	0	$.2653\times10^{-3}$	$.1546\times10^{-3}$	$.1213\times10^{-3}$	$.1106\times10^{-3}$	$.1109\times10^{-3}$
100.0	0	$.2748\times10^{-4}$	$.1742\times10^{-4}$	$.1513\times10^{-4}$	$.1614\times10^{-4}$	$.1962\times10^{-4}$

(b) Re = 100,000.

Pr	$-F_0$	$-F_1$	$-F_2$	$-F_3$	$-F_4$	$-F_5$
0.7	0	0.1947×10^{-2}	0.1034×10^{-2}	0.7110×10^{-3}	0.5407×10^{-3}	0.4400×10^{-3}
1.0	0	$.1375\times10^{-2}$	$.7375\times10^{-3}$	$.5136\times10^{-3}$	$.3963\times10^{-3}$	$.3277\times10^{-3}$
10.0	0	$.1426\times10^{-3}$	$.7971\times10^{-4}$	$.5887\times10^{-4}$	$.4881\times10^{-4}$	$.4403\times10^{-4}$
100.0	0	$.1455\times10^{-4}$	$.8475\times10^{-5}$	$.6375\times10^{-5}$	$.6609\times10^{-5}$	$.5836\times10^{-5}$

(c) Re = 500,000.

Pr	$-F_0$	$-F_1$	$-F_2$	$-F_3$	$-F_4$	$-F_5$
0.7	0	0.4786×10^{-3}	0.2590×10^{-3}	0.1796×10^{-3}	0.1374×10^{-3}	0.1114×10^{-3}
1.0	0	$.3348\times10^{-3}$	$.1818\times10^{-3}$	$.1265\times10^{-3}$	$.9715\times10^{-4}$	$.7893\times10^{-4}$
10.0	0	$.3389\times10^{-4}$	$.1860\times10^{-4}$	$.1312\times10^{-4}$	$.1024\times10^{-4}$	$.8479\times10^{-5}$
100.0	0	$.3401\times10^{-5}$	$.1877\times10^{-5}$	$.1333\times10^{-5}$	$.1048\times10^{-5}$	$.8763\times10^{-6}$

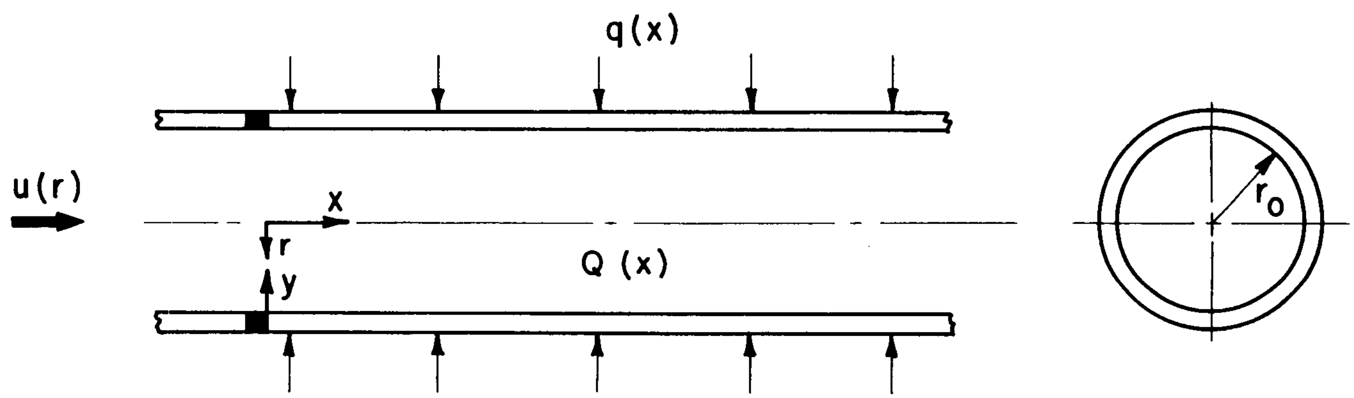

Fig. 1. - Physical model and coordinates.

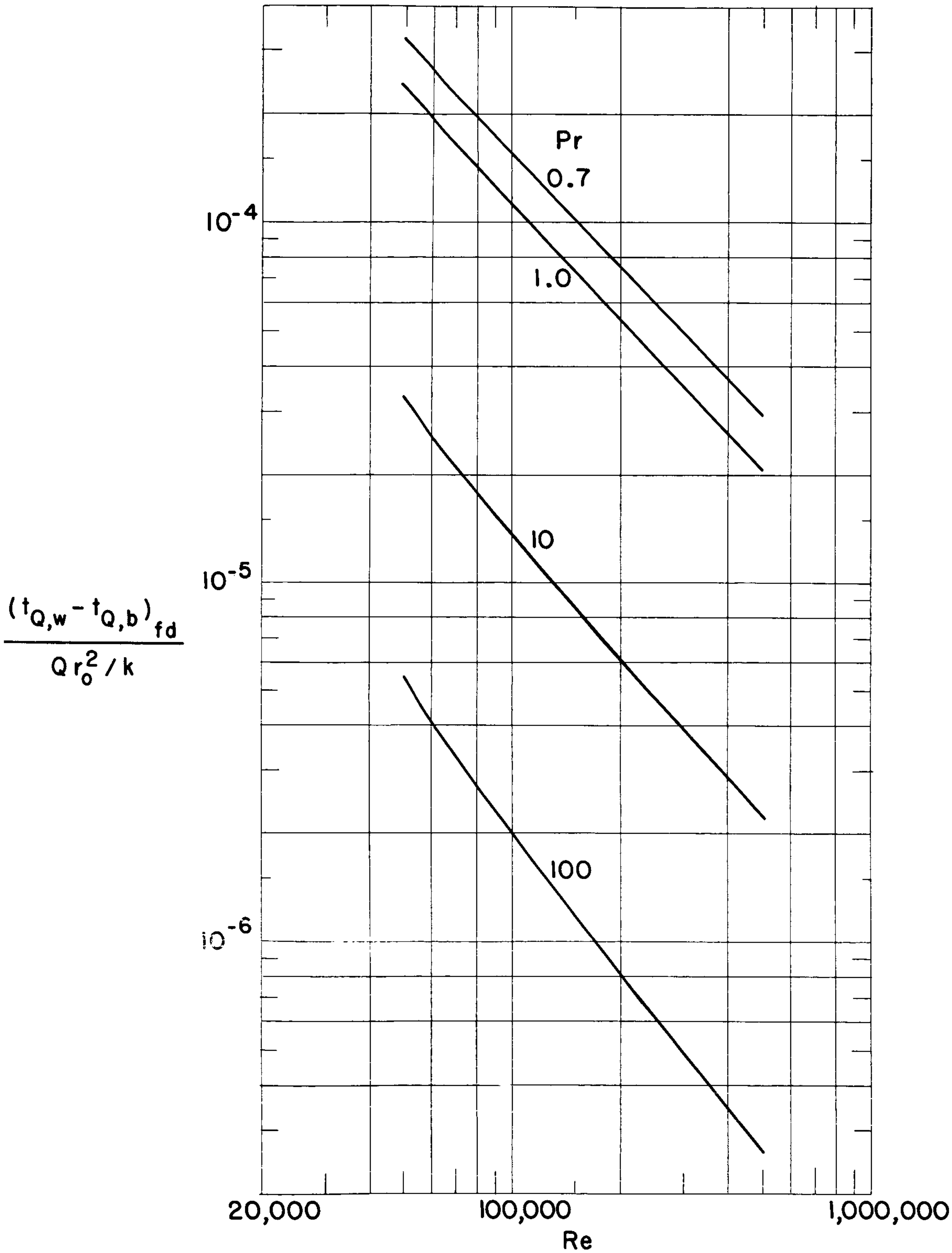

Fig. 2. - Fully developed wall-to-bulk temperature difference for uniform internal heat source in an insulated tube.

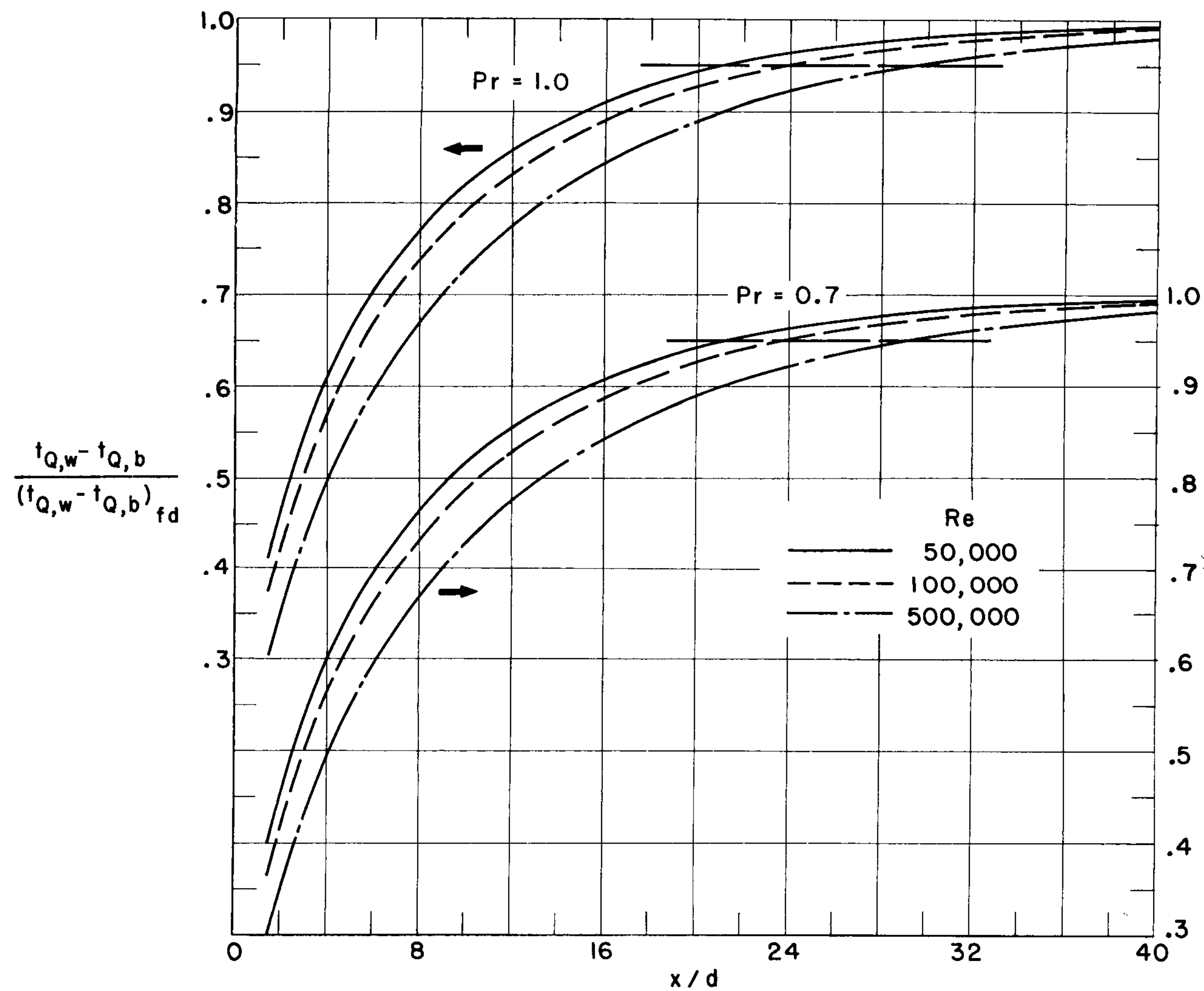

(a) Pr = 0.7, 1.0

Fig. 3. - Wall-to-bulk temperature variation for uniform internal heat source in an insulated tube.

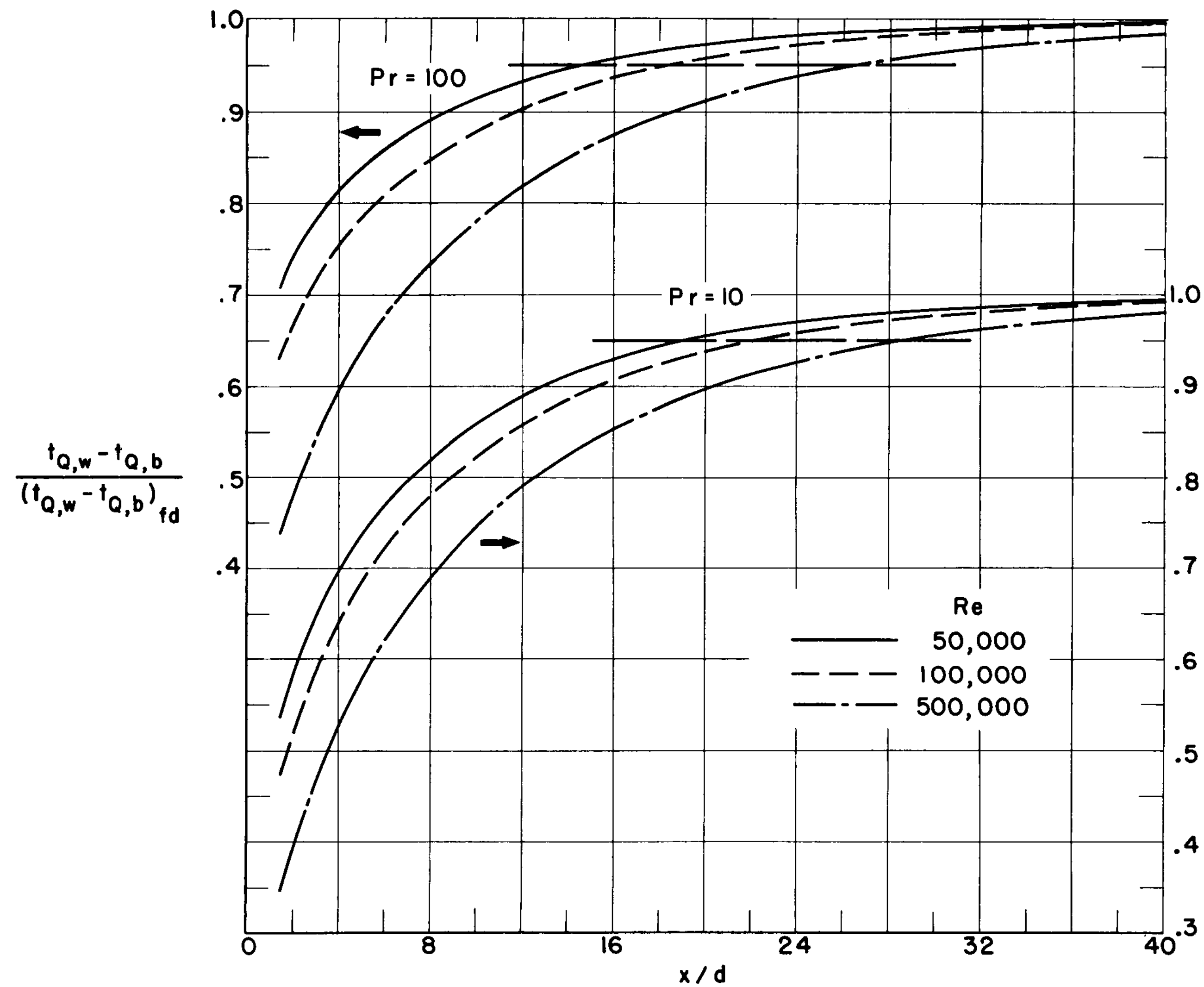

(b) Pr = 10, 100

Fig. 3. - Concluded. Wall-to-bulk temperature variation for uniform internal heat source in an insulated tube.

E-154

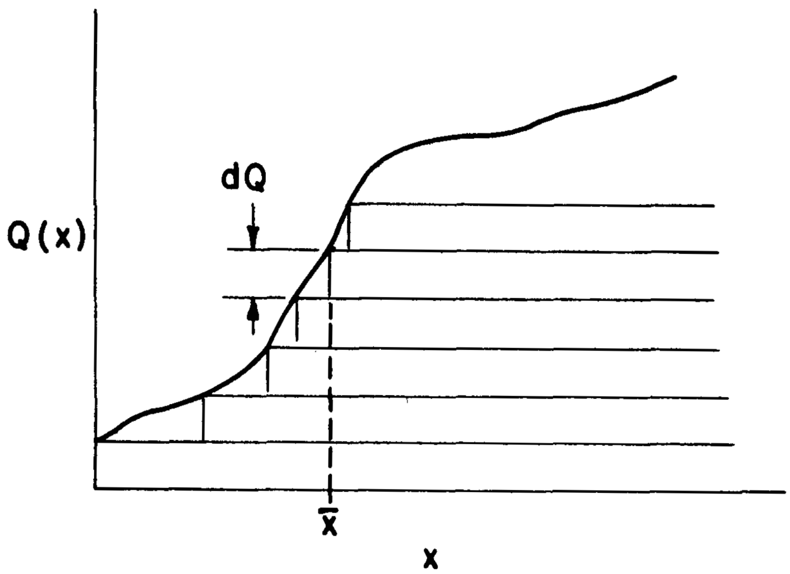

Fig. 4. - Representation of an arbitrary longitudinal internal heat source distribution.

E-154

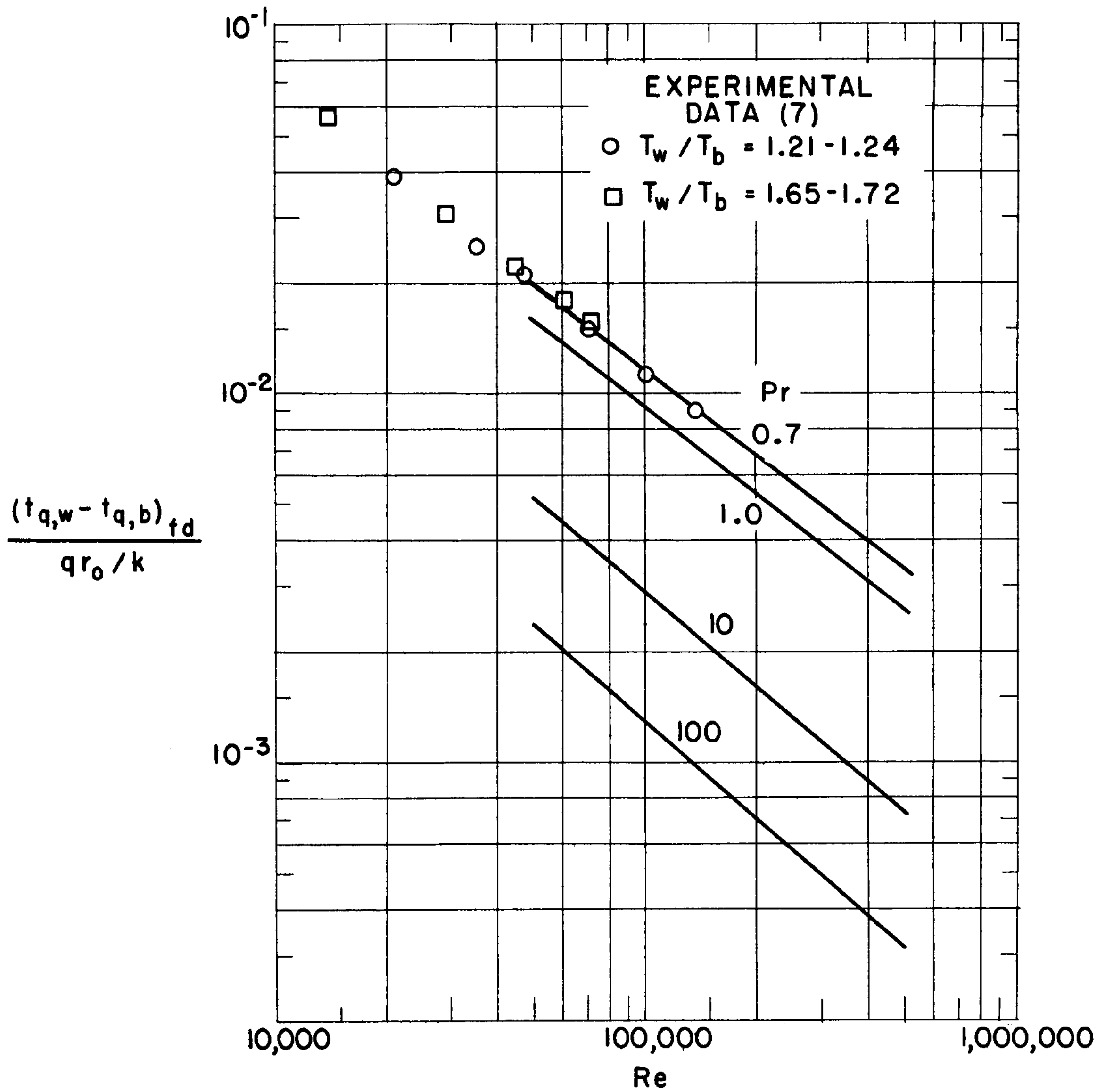

Fig. 5. - Fully developed wall-to-bulk temperature difference for uniform wall heat flux and no internal heat source.

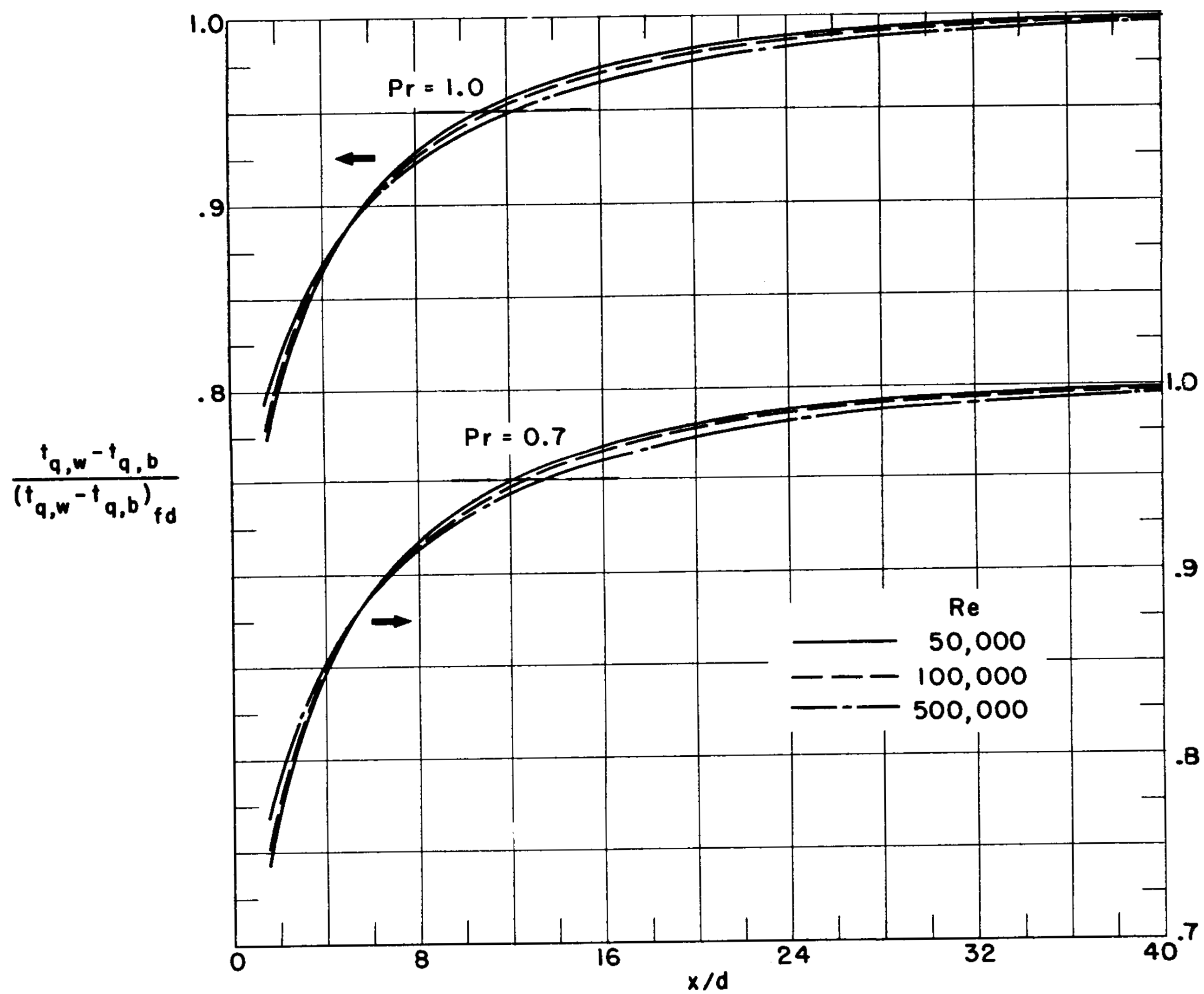

(a) Pr = 0.7, 1.0

Fig. 6. - Wall-to-bulk temperature variation for uniform wall heat flux and no internal heat source.

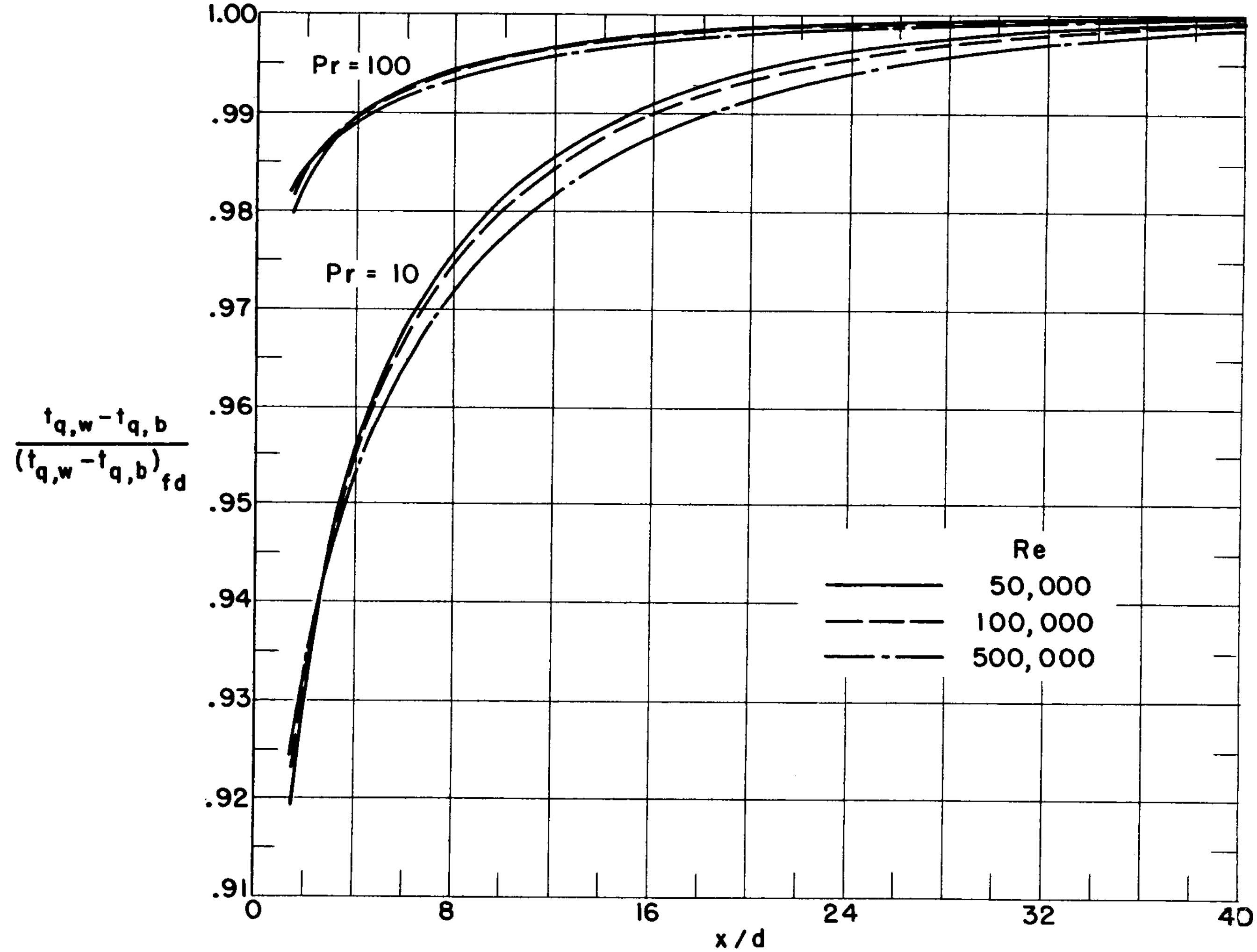

(b) Pr = 10, 100

Fig. 6. - Concluded. Wall-to-bulk temperature variation for uniform wall heat flux and no internal source.